In situ interfacial engineering of 1D Bi_2S_3/2D g-C_3N_4 heterostructure for antibiotics degradation in aqueous media *via* light mediated peroxymonosulfate activation

Muhammad Mateen[a,c]*, Guanrong Chen*[a,b]*, Na Guo*[a,d]**, and Wee Shong Chin*[a,b]*

[a]Advance Manufacturing and Material Center, National University of Singapore (Chongqing) Research Institute, Chongqing, 400000, P. R. China.

[b]Department of Chemistry, Faculty of Science, National University of Singapore, 3 Science Drive 3, 117543, Singapore.

[c]School of Chemistry and Chemical Engineering, Chongqing University, 400000, P. R. China.

[d]Department of Physics, Faculty of Science, National University of Singapore, 3 Science Drive 3, 117543, Singapore.

*Corresponding authors: chmcws@nus.edu.sg (W. S. Chin)
mateenchem@hotmail.com (M. Mateen)
phyguon@u.nus.edu (N. Guo)

1. Supplementary text

S1. Chemicals and materials

Thiourea ($C_3H_6N_6$, 99%), urea (CH_4N_2O, ≥99.0%), and bismuth (III) acetate ($Bi(OCOCH_3)_3$, 98%) were purchased from Alfa Assar. Antibiotics, such as Tetracycline ($C_{22}H_{24}N_2O_8$, ≥98.0%), Sulfamethoxazole ($C_{10}H_{11}N_3O_3S$, 99%), Ciprofloxacin ($C_{17}H_{18}FN_3O_3$, 99.5%), Ofloxacin ($C_{18}H_{20}FN_3O_4$, 99%), Levofloxacin ($C_{18}H_{20}FN_3O_4$, 99%), Rhodamine B ($C_{28}H_{31}ClN_2O_3$, 98%), and Methylene blue ($C_{16}H_{18}ClN_3S$, 98%) were acquired from Shanghai Aladdin Biochemical Technology Co., Ltd. Methanol (CH_4O, 98%), tertiary butyl alcohol ($(CH_3)_3COH$, ≥99.7%), ammonium oxalate ($(NH_4)_2C_2O_4 \cdot H_2O$, ≥99%), 2,2,6,6-tetramethyl piperidine-1-oxyl, TEMPO ($C_9H_{18}NO$, 99%), triethanolamime ($(HOCH_2CH_2)_3N$, 97%), L-histidine ($C_6H_9N_3O_2$, 98.9%), 5,5-dimethyl-1-pyrroline N-oxide ($C_6H_{11}NO$, ≥99.9%), potassium peroxymonosulfate ($KHSO_5 \cdot 0.5KHSO_4 \cdot 0.5K_2SO_4$, 98.5%), and sodium azide (NaN_3 99%), were purchased from Acros Organics Co., Ltd. Sodium chloride (NaCl, 99.9%), Sodium nitrate ($NaNO_3$ 99%), sodium carbonate (Na_2CO_3, 99%), sodium bicarbonate ($NaHCO_3$, 98%), disodium hydrogen phosphate, (Na_2HPO_4), and humic acid sodium salt ($C_9H_8Na_2O_4$, 98%) were bought from Aladdin Reagent Co. Ltd. (Shanghai, China). Deionized water collected by Millipore system was used throughout the reaction.

S2. Synthesis of 1D Bi_2S_3

1D Bi_2S_3 nanostructure was prepared by making minor modifications in previous reported method.[1] In a typical synthesis, bismuth nitrate (0.3mM) and thiourea (0.6mM) were dissolved in 20mL of N, N-dimethylformamide (DMF) in a 50mL glass beaker under stirring for 15 minutes and named as solution A. Solution B was prepared by dissolving 50 mg of polyvinylpyrrolidone

(PVP) in 20 ml of DMF. Next, solution B was added dropwise into solution A under continuous stirring at 100°C. The stirring was kept at the same temperature for 6 hours, while the solution color turned into dark blue. After cooling to indoor temperature, 1D Bi_2S_3 sample was separated by centrifuge at 700RMP. Separation procedure was repeated for three times with ethanol and water and the sample was finally dried at 80°C in an oven for overnight.

S3. Some experimental procedures

S3.1. Characterization techniques

Powder X-ray diffraction data of the prepared photocatalysts was collected on a Bruker D8 High Resolution X–ray diffractometer equipped with Cu Kα irradiation source (λ = 0.1538 nm) at an operating condition of 30 mA and 40 kV with a scan rate (2θ) of 0.01°/sec from 10° to 80°. Scanning electron microscope (SEM) analysis was performed on a Hitachi S-4800 instrument operating at a voltage of 5 keV. Transmission electron microscopy (TEM) images were acquired on a Hitachi SU8010 transmission electron microscope at operating voltage of 100kV. High angle annular dark field scanning transmission electron microscopy (HAADF-STEM) analysis and elemental mapping was executed on FEI Tecnai G2 F20 S-TWIN instrument coupled with energy dispersive X-ray spectroscopy (EDS) detector system at an operating voltage of 200 kV. For surface elemental composition and electronic structure analysis X–ray photoelectron spectroscopic (XPS) data was acquired on ESCALAB 250Xi X-ray photoelectron spectrometer equipped with monochromatized Al Kα X–ray source, and binding energies were calibrated with reference to C 1s at 284.6 eV. The UV–Vis diffuse reflectance spectroscopic analysis of as prepared photocatalysts was performed on Shimadzu UV–2450, spectrometer) in the 200–800 nm range using $BaSO_4$ as the reflectance standard material. The PL emission spectra were recorded on a F–

7000, HITACHI, (Japan) Spectrofluorometer at exciting wavelength of 450 nm provided by a Xenon lamp. Fourier transform infrared (FT–IR) spectra were recorded on IRPrestige–21, Shimadzu, (Japan) in the range of 4000–400 cm^{-1} using KBr as the reference.

S3.2. Photoelectrochemical measurements

The photocurrent response and electrochemical impedance spectroscopy (EIS) of g-C_3N_4, Bi_2S_3 and Bi_2S_3*(0.2)*/g-C_3N_4, were inspected on a CHI 660E electrochemical workstation (Ch Instruments, Shanghai, China) using standard three-electrode model at constant potential of -0.2 V (*vs.* SCE), where Pt wire served as the counter electrode, KCl saturated Ag/AgCl electrode as the reference electrode, and 0.2M Na_2SO_4 aqueous solution as the electrolyte. The working electrodes for g-C_3N_4, Bi_2S_3 and Bi_2S_3*(0.2)*/g-C_3N_4 were prepared as follows: 20mg of the photocatalyst was dispersed in 1mL ethanol, then sonicated to make a slurry after adding 20 μL of 0.5% Nafion solution. Next, 50μL of the prepared slurry was casted onto a 2cm × 2cm FTO glass film and dried in vacuum oven at 80◦C.

S3.3. Procedure for studying the degradation of antibiotics

Typically, catalytic experiments for the degradation experiments of organic pollutants (antibiotics and dyes) was carried out in a 50 mL beaker. In details, 30mg of the prepared photocatalyst was dispersed into 50mL solution containing 20mg/L pollutants (TC, CIP, LEV, OX, SMX, RhB, MB) and the solution pH was then adjusted to 7 using 0.5M H_2SO_4 or NaOH. Then, the mixture was kept under stirring in the dark for 30 min to attain the adsorption–desorption equilibrium. Next, after adding 2mM of peroxymonosulfate (PMS) into the suspension, the reaction system was immediately exposed to light provided by a 300W Xe lamp with UV cutoff filter of λ=420 nm. At

regular interval of 10 minutes, 3mL of reaction mixture was sampled and filtered using a 0.45 μm syringe filter to separate aqueous solution and the solid catalyst. The temporal concentration of pollutants during 60 minutes of irradiation was determined through recording the characteristic absorption spectra of TC (357nm), CIP (276nm), LEV (286nm), SMX (262nm), OX (288nm), RhB (567nm), and MB (665nm) on a UV600 Shimadzu spectrophotometer. Control experiments were conducted without adding PMS, without adding photocatalysts, and under dark conditions. Kinetic rate constant (*k*) values for the prepared photocatalysts were evaluated by applying pseudo-first order reaction equation:

$$-\ln(C_o/C_t) = kt \qquad (S1)$$

Meanwhile, the % degradation efficiency was calculated by the following equation:

$$\%\ removal\ efficiency = (C_o - C_t/C_o) \times 100 \qquad (S2)$$

Where the abbreviations C_o, C_t, k, and t in equation S1 and S2 corresponds to initial concentration, concentration at time t, first-order kinetic rate constant, and reaction time(minutes), respectively. To assess the contribution of various radicals and non-radicals species during the degradation, co-quenching experiments were performed by adding tert-butyl alcohol (TBA, $^{\bullet}OH$), ethanol (EtOH, $^{\bullet}OH$ and $SO_4^{\bullet-}$), triethanolamine (TEO, h^+), L-histidine (L-His, $^1O_2$), and 2,2,6,6-tetramethylpiperidine-1-oxyl (TEMPOL, $O_2^{\bullet-}$), and sodium azide (NaN_3,$^{\bullet}OH$, $SO_4^{\bullet-}$, $^1O_2$, and $O_2^{\bullet-}$). To study the pH effect, the solution pH was adjusted from 1 to 9 with the help of 1M NaOH and 0.2M H_2SO_4 solution. Interference of various ions (Cl^-, NO_3^-, HPO_4^{2-}, CO_3^{2-} and HCO_3^-) and organic matter was investigated by adding respectively 2mM, 5mM and 10mM of NaCl, $NaNO_3$, Na_2CO_3, $NaHCO_3$, Na_2HPO_4, and sodium salt of humic acid.

S4. Theoretical computation

The first-principles calculations were performed with spin-polarized density functional theory (DFT) by utilizing Vienna ab-initio Simulation Package (VASP).[2,3] The generalized gradient approximation (GGA) in the Perdew-Burke-Ernzerhof (PBE) format and the projector-augmented wave (PAW) method were employed in all calculations. [4-6] A plane wave basis with the cut-off energy of 450 eV was applied. Van der Waals force (DFT+D3) was included in the geometry relaxation and molecule adsorption simulations (O_2, SO_4 and HO-SO_4).[7] The convergence criterion was set to less than 10^{-5} eV and 0.01 eV/Å for the total energy and the residual Hellmann-Feynman force acting on each atom, respectively. Gamma-point sampling was adopted in all calculations. The g-C_3N_4 substrate was modeled as a 5×5 supercell in the heterostructure with a vacuum layer of 20 Å in the direction perpendicular to g-C_3N_4 sheet to avoid artificial interaction between the neighboring images. The 9x1x1 supercell of 1DBi_2S_3 molecular chain was chosen in the study to keep the lattice mismatch of the heterostructure less than 3%.

2. Supplementary figures

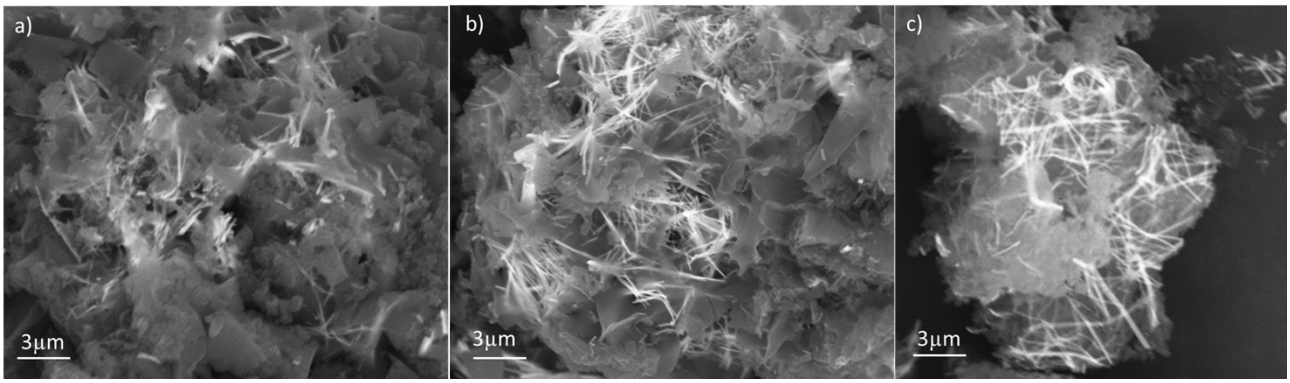

Figure S1: FE-SEM images of a) 1DBi_2S_3*(0.1)*/2Dg-C_3N_4, b) 1D Bi_2S_3*(0.2)*/2Dg-C_3N_4 and c) 1DBi_2S_3*(0.3)*/2Dg-C_3N_4.

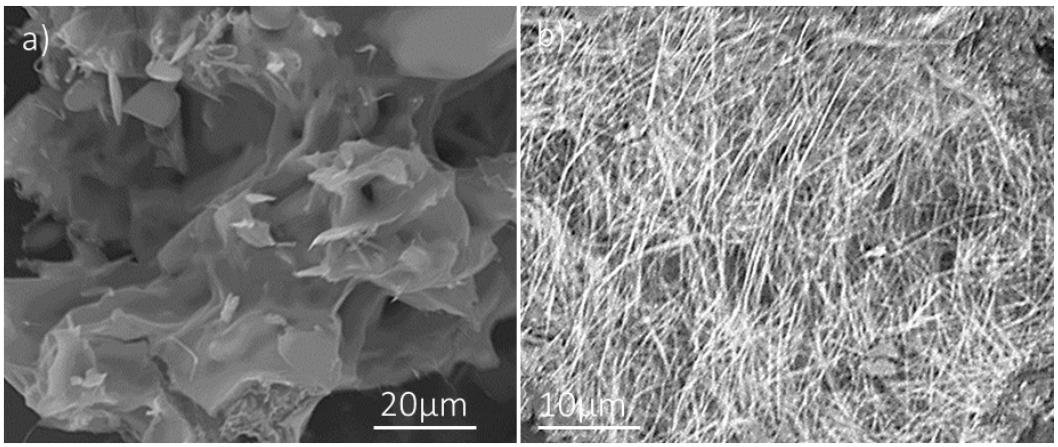

Figure S2: FE-SEM and TEM images of, a) pristine 2Dg-C_3N_4 and b) pristine 1DBi_2S_3.

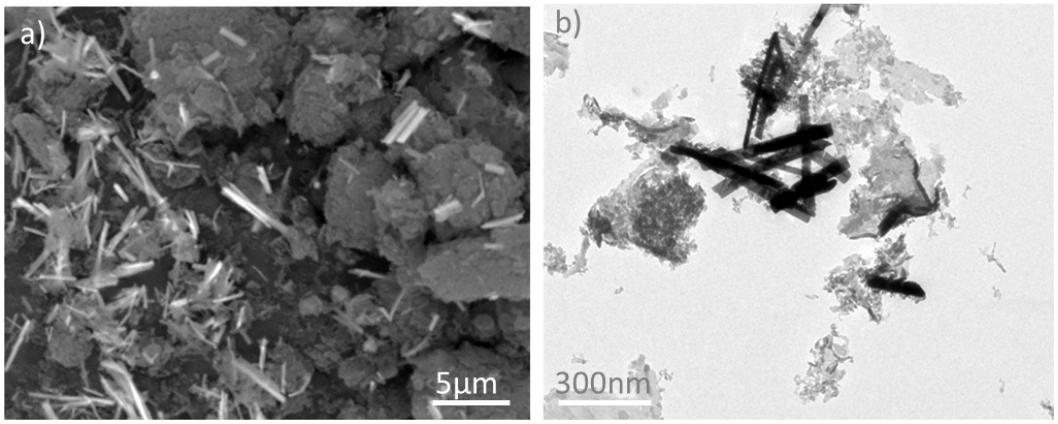

Figure S3: a) FE- SEM image and b) TEM image of physically prepared 1DBi_2S_3/2Dg-C_3N_4 heterostructure.

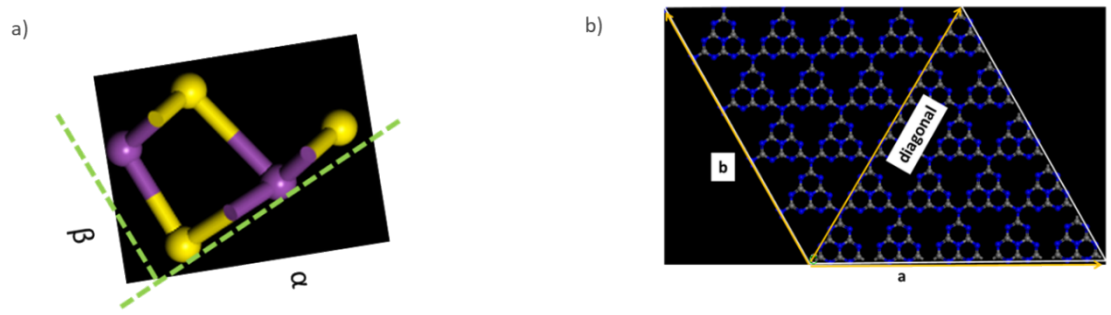

Figure S4. a) α and β facets of optimized DFT 1D Bi_2S_3 model, and b) various possible directions: a, b, or diagonal, for placing 1D Bi_2S_3 chains over 2D g-C_3N_4 surface.

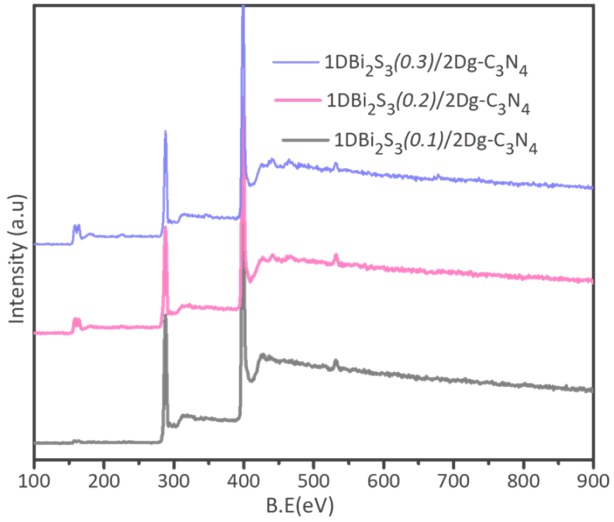

Figure S5. XPS survey scan spectra of the prepared 1DBi_2S_3*(n)*/2Dg-C_3N_4 heterostructures.

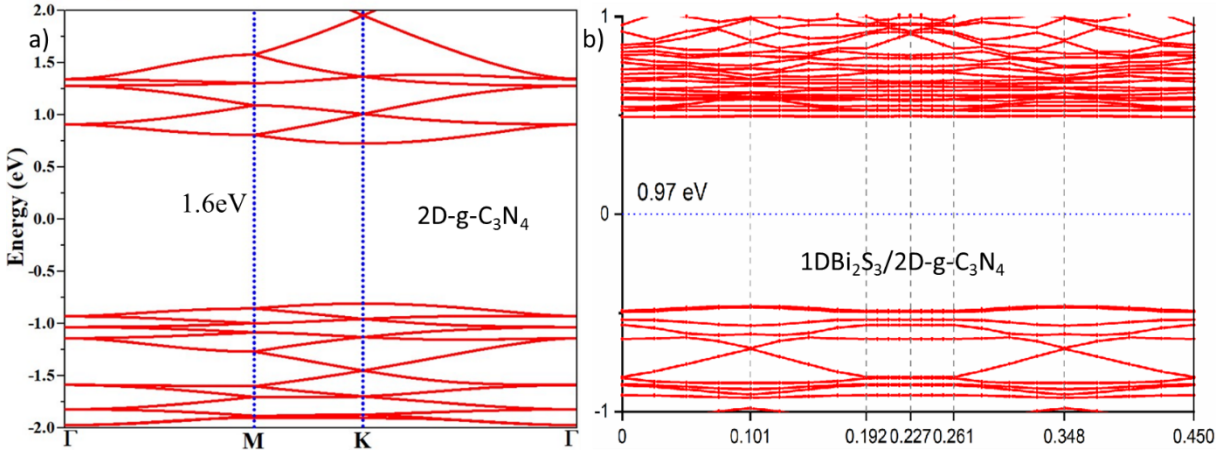

Figure S6. Energy band structures calculated for a) 2D-gC_3N_4 and b)1D Bi_2S_3/2Dg-C_3N_4.

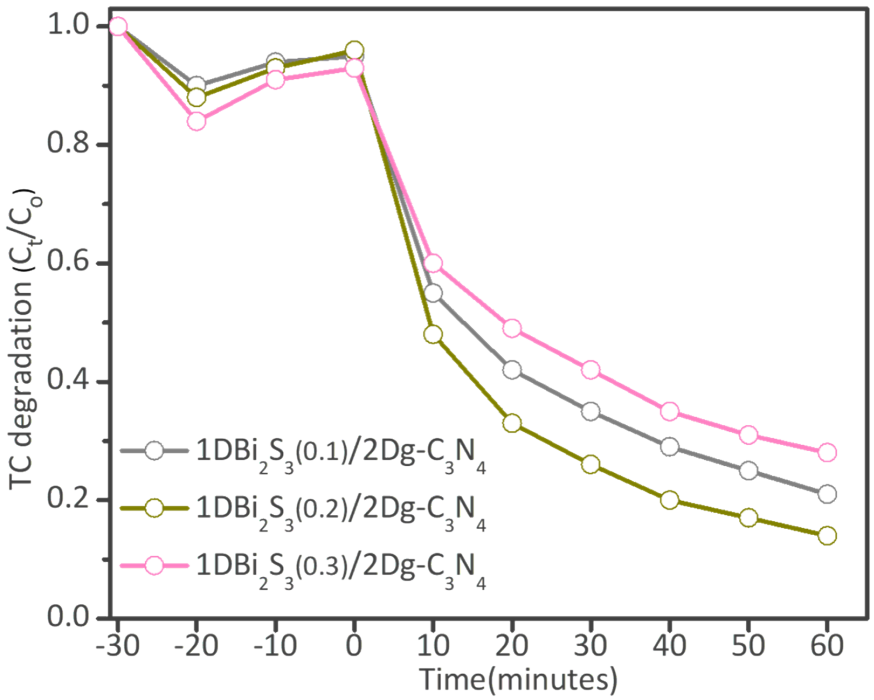

Figure S7. Tetracycline (TC) degradation catalyzed by $1DBi_2S_3(n)/2Dg\text{-}C_3N_4$ heterostructures (where n=0.1,0.2 and 0.3) under visible-light. (Reaction condition: [TC] = 20 mg L^{-1}, [catalyst] = 30mg and pH = 7.0).

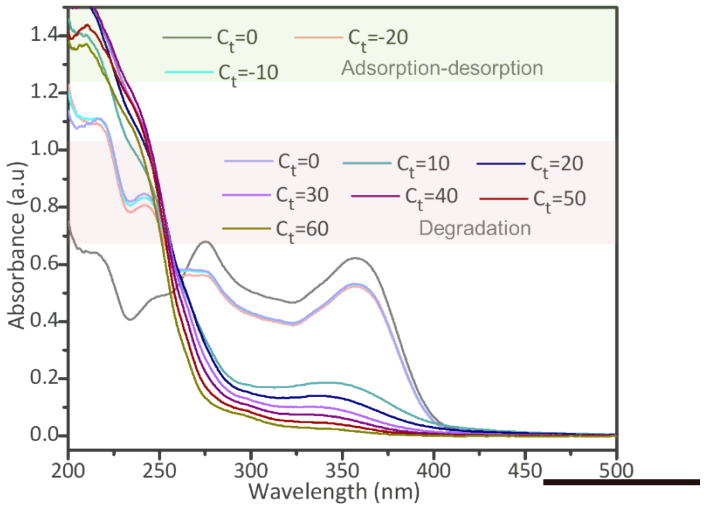

Figure S8. UV-visible spectra of tetracycline degradation on $1DBi_2S_3(0.2)/2Dg\text{-}C_3N_4$ heterostructure with added PMS under visible-light. (Reaction condition: [TC] = 20 mg L^{-1}, [catalyst] = 0.2 g and pH = 7.0).

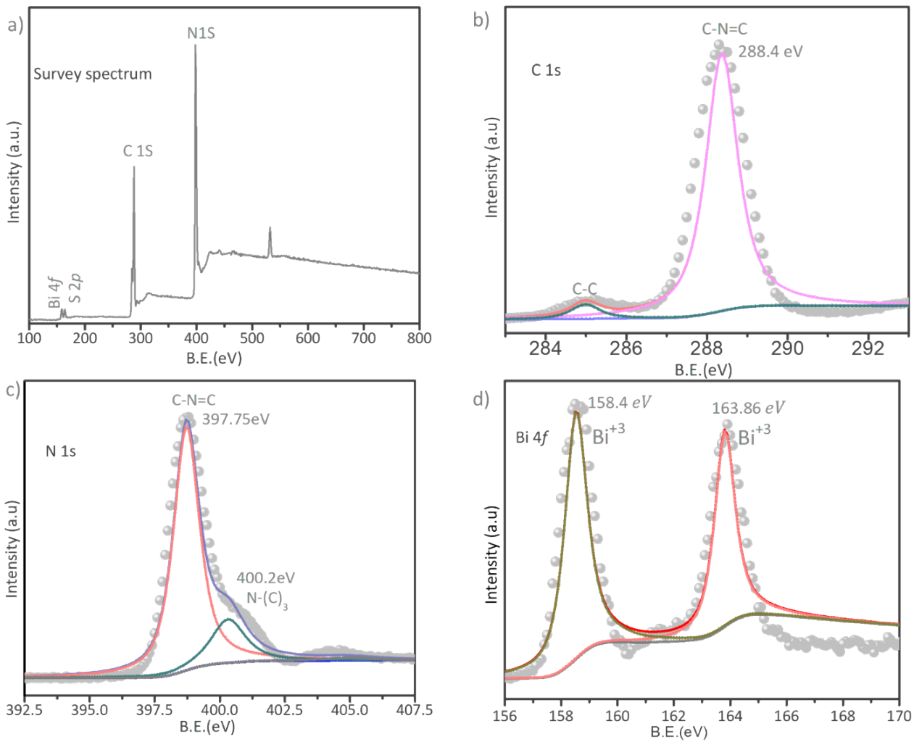

Figure S9. XPS analysis of physically mixed $1DBi_2S_3$ and $2Dg\text{-}C_3N_4$ composite: a) Survey scan of $Bi_2S_3/g\text{-}C_3N_4$ heterostructure, b) C 1s spectrum, c) N 1s spectrum and d) Bi 4f spectrum.

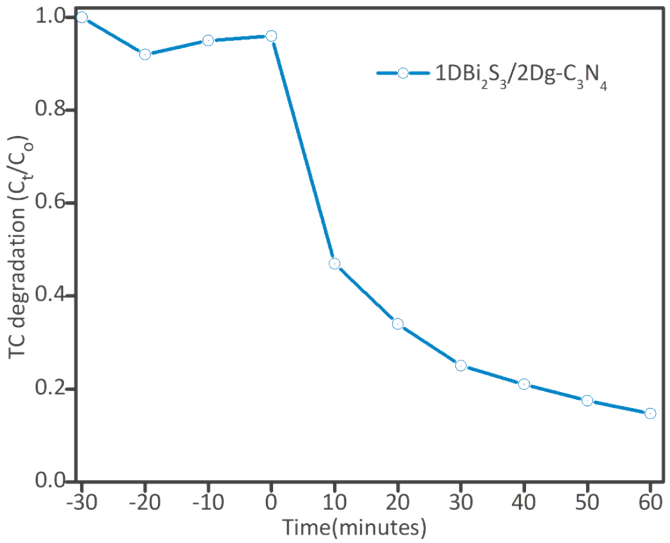

Figure S10. Degradation of tetracycline on physically mixed $1DBi_2S_3/2Dg\text{-}C_3N_4$ composite under visible-light and with added PMS. (Reaction condition: [TC] = 20 mg L^{-1}, [catalyst] = 30mg, [PMS] = 2mM and [pH] = 7.0).

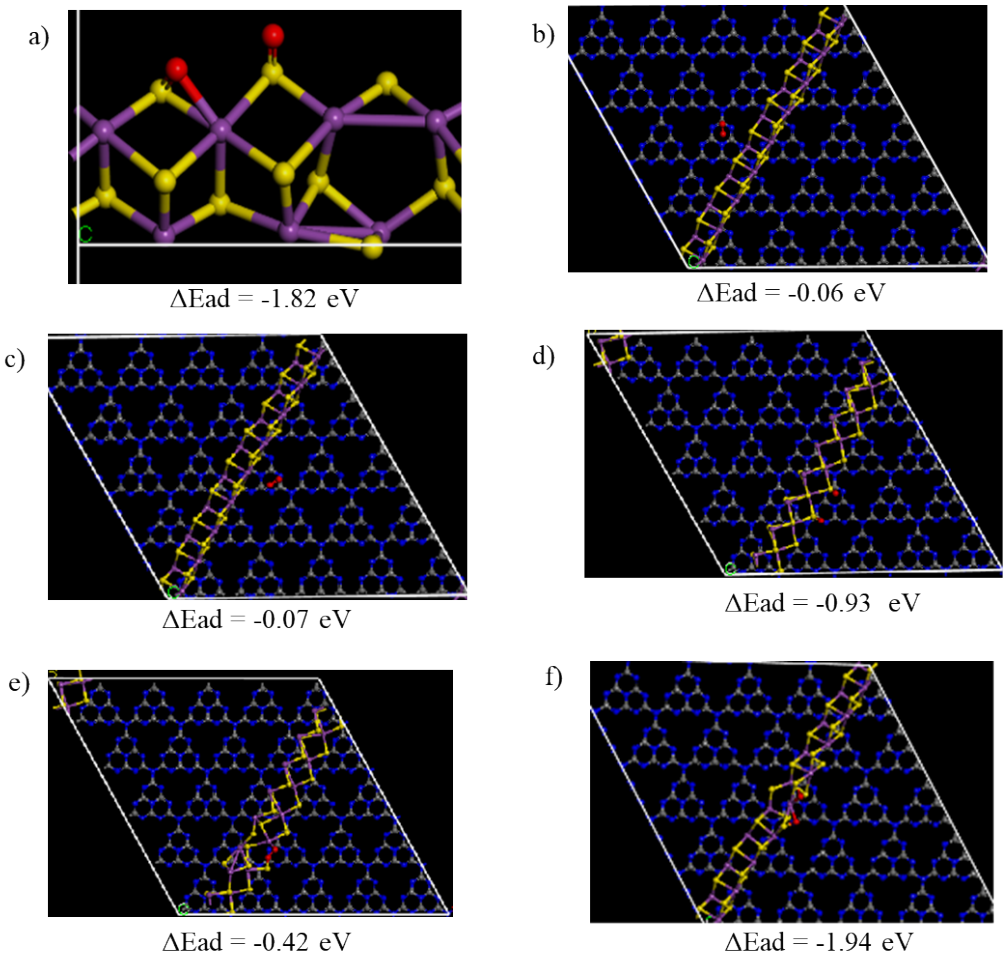

Figure S11. DFT optimized configurations for O_2 adsorption on: a) $1DBi_2S_3$, b) $1DBi_2S_3$/2Dg-C_3N_4-α (g-C_3N_4 site), c) $1DBi_2S_3$/2Dg-C_3N_4-β (g-C_3N_4 site), d) $1DBi_2S_3$/2Dg-C_3N_4-α (S site), e) $1DBi_2S_3$/2Dg-C_3N_4-α (Bi site) and f) $1DBi_2S_3$/2Dg-C_3N_4-β (S site).

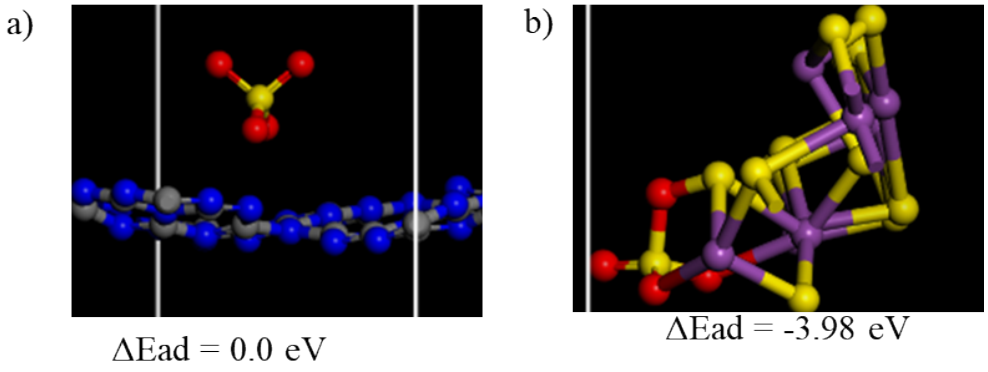

Figure S12. PMS adsorption on a) 2Dg-C_3N_4 and b) 1D Bi_2S_3.

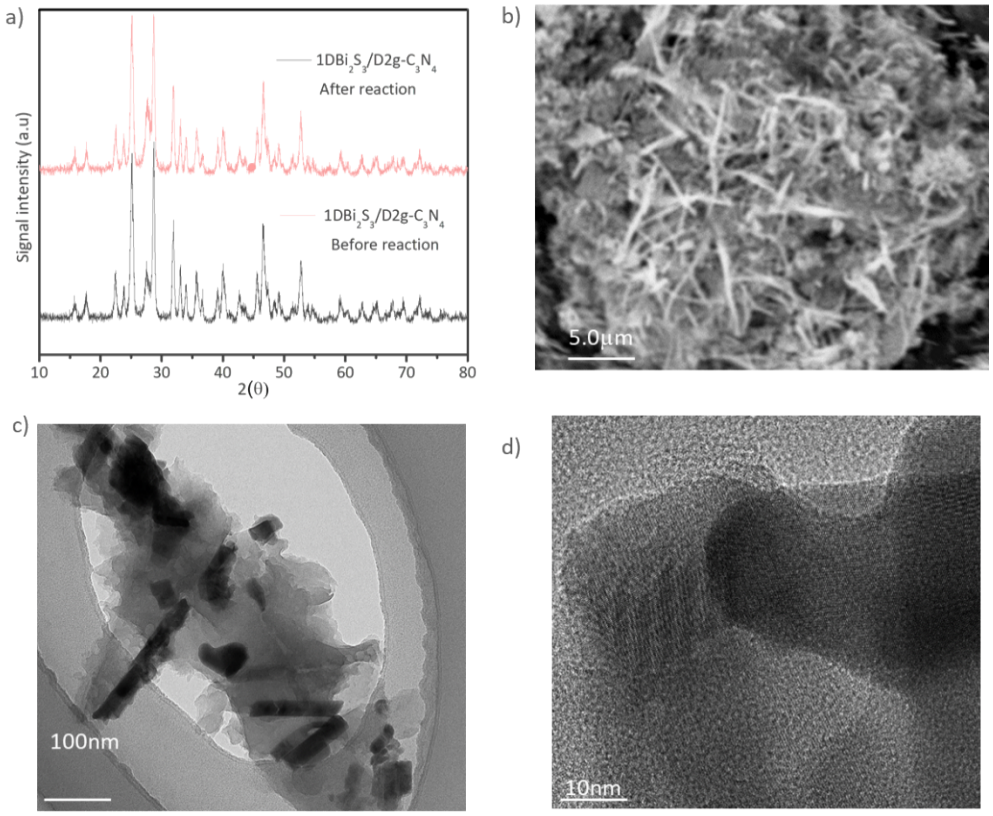

Figure S13. Post catalysis characterizations of $1DBi_2S_3$*(0.2)*/2Dg-C_3N_4: a) powder XRD pattern, b) SEM image, c) TEM image and d) HR-TEM image.

References

S1. J. Arumugam, Amal George, A. Dhayal Raj, A. Albert Irudayaraj, R.L. Josephine, S. John Sundaram, Amal M. Al-Mohaimeed, Wedad A. Al-onazi, Mohamed Soliman Elshikh, K. Kaviyarasu. Construction and Characterization of Photodiodes prepared with Bi_2S_3 Nanowires. *J. Alloys Compd.* **2011**, 863, 158681.

S2. Kresse G, Furthmüller J. Efficient iterative schemes for ab initio total-energy calculations using a plane-wave basis set. Phys. Rev. B. **1996**, 54(16),11169.

S3. Kresse G, Hafner J. Ab initio molecular dynamics for liquid metals. Phys. Rev. B. **1993,** 47(1),558.

S4. Henkelman G, Uberuaga BP, Jónsson H. A climbing image nudged elastic band method for finding saddle points and minimum energy paths. J. Chem. Phys., 2000, 113(22): 9901–9904.

S5. Perdew JP, Burke K, Ernzerhof M. Generalized gradient approximation made simple. Phys. Rev. Lett. **1996**, 77(18), 3865.

S6. Blöchl PE. Projector augmented-wave method. *Phys. Rev. B.* **1994**, 50(24), 17953.

S7. Grimme, S., Ehrlich, S. & Goerigk, L. Effect of the damping function in dispersion corrected density functional theory. *J. Comput. Chem.* **2011**, 32, 1456–1465.

S8. Min Wang, Chongyue Jin, Zhilin Li, Meiyan You, Yu Zhang, Tong Zhu. The effects of bismuth (III) doping and ultrathin nanosheets construction on the photocatalytic performance of graphitic carbon nitride for antibiotic degradation. *J. Colloid Interface Sci.* 2019, 533, 513–525

S9. Dongdong Chen, Jianzhang Fang, Shaoyou Lu, GuangYing Zhou, Weihua Feng, Fan Yang, Yi Chen, ZhanQiang Fang Fabrication of Bi modified Bi_2S_3 pillared g-C_3N_4 photocatalyst and its efficient photocatalytic reduction and oxidation performances. *Appl. Surf. Sci*, **2017**, 426, 427-436'

S10. Poulomi Sarkar, Sudarsan Neogi, Sirshendu De. Activation of peroxymonosulfate by S-scheme Bi_2S_3/doped g-C_3N_4 heterostructure photocatalyst for highly efficient visible light driven tetracycline degradation: Insights into reaction mechanisms. *Sep. Purif. Technol*. **2023**, 308, 122908.

S11. Qiong Wu, Dingze Lu, Kiran Kumar Kondamareddy, Wingkei Ho, Dezhong Cao, Yimei Zeng, Boyu Zhang, Yuhao Zhang, Lihao Xie, Bang Zhao, Zhennan Wang, Hongjuan Hao, Huiqing Fan, Hongmei Wang. *Arab. J. Chem*. **2022**, 2022, 103689.

S12. Hui Liu, Wangchen Huo, Tian C. Zhang, Like Ouyang. Shaojun Yuan aPhotocatalytic removal of tetracycline by a Z-scheme heterojunction of bismuth oxyiodide/exfoliated g-C_3N_4: performance, mechanism, and degradation pathway. *Mater. Today Chem*. *2023*, 22, 100729.

S13. Chenyu Wu, Huiru Zuo, Haoyu Du, Siyu Zhang, Lingrui Wang, Qishe Yan Construction of layered embedding dual Z-Scheme $Bi_2O_2CO_3$/g-C_3N_4/Bi_2O_3: Tetracycline degradation pathway, toxicity analysis and mechanism insight. *Sep. Purif. Technol*., 2022, 282, 120096.

S14. Chao Yin, Yali Liu, Xinya Lv, Shuyi Lv, Han cheng, Xiaorong Kang, Xin Li Carbon dots as heterojunction transportmediators effectively enhance BiOI/g-C_3N_4 synergistic persulfate degradation of antibiotics. *Appl. Surf. Sci*. **2022**, 601, 154249.

S15. Longbo Jiang, Xingzhong Yuan, Guangming Zen, Jie Liang, Xiaohong Chen, Hanbo Yu, Hou Wang, Zhibin Wu, Jin Zhang, Ting Xiong. In-situ synthesis of direct solid-state dual Z-scheme WO_3/g-C_3N_4/Bi_2O_3 photocatalyst for the degradation of refractory pollutant. *Appl. Catal. B Environ.* **2018**, 227, 376-385.

S16. Wei Liu, Zhaohua Li, Qun Kang, Lilian Wen. Efficient photocatalytic degradation of doxycycline by coupling α-Bi_2O_3/g-C_3N_4 composite and H_2O_2 under visible light. *Environ. Res*. **2021**,197, 110925.

S17.Zhun Shi, Yan Zhang, Xiaofeng Shen, Gumila Duoerkun, Bo Zhu, Lisha Zhang, Maoquan L, Zhigang Chen, Fabrication of g-C_3N_4/BiOBr heterojunctions on carbon fibers as weaveable photocatalyst for degrading tetracycline hydrochloride under visible light. *Chem. Eng. J*. **2020**, 386, 124010.

S18. Dongling Jia, Yifan Zhang, Xue Zhang, Peiying Feng, Lin Yang, Ruonan Ning, Hongzhi Pan and Yuqing Miao. Facile fabrication of Bi nanoparticle-decorated g-C_3N_4 photocatalysts for effective tetracycline hydrochloride degradation: environmental factors, degradation mechanism, pathways and biotoxicity evaluation. *Environ. Sci.: Nano***. 2021**,8, 415-431.

S19. Dongdong Chen, Shuxing Wu, Jianzhang Fang, Shaoyou Lu, GuangYing Zhou, Weihua Feng, Fan Yang, Yi Chen, ZhanQiang Fang. A nanosheet-like α-Bi_2O_3/g-C_3N_4 heterostructure modified by plasmonic metallic Bi and oxygen vacancies with high photodegradation activity of organic pollutants. *Sep. Purif. Technol*. **2018**, 193, 232−241.

S20. Huinan Che, Chunbo Liu, Wei Hu,a Hao Hu, Jinqiao Li, Jianying Dou, Weidong Shi, Chunmei Li, Hongjun Dong. NGQD active sites as effective collectors of charge carriers for improving the photocatalytic performance of Z-scheme g-C_3N_4/Bi_2WO_6 heterojunctions. *Catal. Sci.Technol*. **2018**, 8, 622−631.

S21. Lijia Huang, Hui Liu, Yuan Wang, Tian C. Zhang, Shaojun Yuan. Construction of ternary Bi_2O_3/biochar/g-C_3N_4 heterojunction to accelerate photoinduced carrier separation for enhanced tetracycline photodegradation. *Appl. Surf. Sci.* **2023**, 616, 156509.

S22. Gaurav Sharma, Amit Kumar, Shweta Sharma, Mu. Naushad, Dai-Viet N. Vo, Mohd Ubaidullah, Sabry M. Shaheen, Florian J. Stadler. Visible-light driven dual heterojunction formed between g-C_3N_4/BiOCl@MXene-Ti_3C_2 for the effective degradation of tetracycline. *Environ. Pollut*. 2022,308, 119597.

S23. Yizhu Wang, Zipeng Xing, Yi Yang, Weifeng Kong, Chunxu Wu, Hui Peng, Zhenzi Li, Ying Xie, Wei Zhou. Oxygen-defective Bi_2MoO_6/g-C_3N_4 hollow tubulars Sscheme heterojunctions toward optimized photocatalytic performance. *J. Colloid Interface Sci.* **2024**, 653, 1566-1576.

S24. Dongdong Chen, Lina Li, Lixuan Zhuang, Yujun Liu, Bo Zhang, Zhenzhen Jia. Highly efficient CoFe LDO/α-Bi_2O_3/g-C_3N_4 heterojunction forphotocatalytic elimination of antibiotic pollutants. *Appl. Catal. O: Open*. **2024**, 194, 206992.
S25. Ganghua Zhou, Lirong Meng, Xin Ning, Weiqin Yin, Jianhua Hou, Qiao Xu, Jianjian Yi, Shengsen Wang, Xiaozhi Wang. Switching charge transfer of g-C_3N_4/$BiVO_4$ heterojunction from type II to Z-scheme via interfacial vacancy engineering for improved photocatalysis. *Int. J. Hydrogen Energ*. **2022**, 47, 8749-8760.
S26. Feng Guo, Weilong Shi, Huibo Wang, Hui Huang, Yang Li, Zhenhui Kang. Fabrication of a $CuBi_2O_4$/g-C_3N_4 p–n heterojunction with enhanced visible light photocatalytic efficiency toward tetracycline degradation. *Inorg. Chem. Front.* **2017**, 4, 1714-1720.
S27. Min Liu, Hailan Qin, Haiming Xu, Zhongwei Zou, Chengming Deng, Dongsheng Xia, Qilin Yu, Yi Zheng, Dahong Chen. Confine activation peroxymonosulfate by surface oxygen vacancies of $BiO_{1-x}Cl$ to boost its utilization rate. *Sep. Purif. Technol.***2023**, 307, 122711.
S28. Jin Kang, Yiwu Tang, Min Wang, Chongyue Jin, Jiayun Liu, Siyan Li, Zhilin Li, Jiangwei Zhu. The enhanced peroxymonosulfate-assisted photocatalytic degradation of tetracycline under visible light by g-C_3N_4/Na-$BiVO_4$ heterojunction catalyst and its mechanism. *J. Environ. Chem. Eng*. **2021**, 9, 105524.
S29. Ruyao Chen, Xincheng Dou, Jiazeng Xia, Yigang Chen, Haifeng Shi. Boosting peroxymonosulfate activation over Bi_2MoO_6/$CuWO_4$ to rapidly degrade tetracycline: Intermediates and mechanism. *Sep. Purif. Technol.* **2022**, 296, 121345.
S30. Gubran Alnaggar, Abdo Hezam, Q.A. Drmosh, Sannaiah Ananda. Sunlight-driven activation of peroxymonosulfate by microwave synthesized ternary MoO_3/Bi_2O_3/g-C_3N_4 heterostructures for boosting tetracycline hydrochloride degradation. *Chemosphere*, **2021**, 272, 129807.
S31. Zhenzong Zhang, Ziwei Pan, Yongfu Guo, Po Keung Wong, Xiaoji Zhou, Renbi Bai. In-situ growth of all-solid Z-scheme heterojunction photocatalyst of $Bi_7O_9I_3$/g-C_3N_4 and high efficient degradation of antibiotic under visible light. *Appl. Catal. B Environ*. **2020**, 261, 118212.